INTERNATIONAL JOURNAL OF OPTIMIZATION IN CIVIL ENGINEERING
Int. J. Optim. Civil Eng., 2021; 11(3):515-546

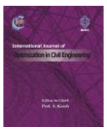

THE EFFECT OF NON-LINEAR FINITE ELEMENT ANALYSIS ON THE DESCRIPTION OF THE GLOBAL BEHAVIOR OF A PREFABRICATED RC SKELETON

Z. Roszevák[*, †] and I. Haris
Department of Structural Engineering, Budapest University of Technology and Economics, Budapest, Hungary

ABSTRACT

Nowadays, the behavior of designed structures is mostly studied using numerical software products. It is important that the models are sufficiently simple, but the calculated values approximate well the real behavior of the structures. In order for a numerical model to realistically describe the structural behavior, the software used must have material models that are parametrized accordingly. The primary purpose of this article is to create various prefabricated reinforced concrete specific joints in a simply prefabricated RC frame. Thus, in the present study, we examined prefabricated column-cup foundation and column-beam connections. The numerical analyses were carried out in the ATENA 3D software, in which the modeling technique we have developed can be used to examine reinforced concrete structures and structural details at a high level. In these studies, we highlight the differences between linear and nonlinear numerical methodologies. During our investigations, we analyze the joints of the examined frame in separate models on which we operate monotonically increasing vertical and horizontal loads. We examine the obtained load-displacement graphs, the failure of the connections, and the behavior of the elements that make up each connection.

Finally, we extended the relationship by modeling the beam of the frame position, pointing out the behavior of the entire structure.

Keywords: precast beam-column connection; precast cup foundation; pocket foundation; nonlinear finite element analysis; ATENA 3D software.

Received: 10 June 2021; Accepted: 23 August 2021

[*]Corresponding author: Department of Structural Engineering, Budapest University of Technology and Economics, Budapest, Hungary
[†]E-mail address: roszevak.zsolt@emk.bme.hu (Z. Roszevák)

1. INTRODUCTION

As a result of industrialization and the rapid developments of the last century, the use of precast reinforced concrete structures in construction has become increasingly common. With prefabricated elements, the high quality of manufactured elements can be ensured. The need for “live labor” on site can be significantly reduced and much faster construction can be achieved compared to cast-in-situ RC structures. The disadvantage is that the design and construction of the appropriate design of the connections between prefabricated - cast-in-situ and prefabricated - prefabricated structural elements requires a great deal of experience. The implementation of improper, poorly constructed joints can cause serious structural problems, damage and even failure. The proper design of junctions is one of the most important tasks in the construction of precast (and cast-in-situ) RC structures, since the response of the whole structure to loads depends on the behavior of the system of established connections. In addition, the joints specified in the design may differ in construction, and construction and manufacturing defects may also appear. With the modeling procedure developed by us, we can examine the effect of possible construction and manufacturing errors by parameterizing. With all this in mind, within the framework of this article, we deal with the modeling and the behavior of a prefabricated RC pocket foundation and frame-corner joint. In the course of our investigations, we examined the joint design of a simple framework, which is modeled in a hinge and a perfectly rigid way in the design software during everyday design. One of the most common finite element software products in Hungary is Axis VM, in which we also examined the frame structure with the dimensions we defined. In AxisVM we performed a simple linear finite element calculation, the elements were modeled with simple two-dimensional beam elements. The joint details of this framework were examined with a higher level three-dimensional nonlinear finite element program. We performed our numerical test in the ATENA 3D nonlinear finite element software, with which the structural details of reinforced concrete can be examined with sufficient accuracy using the modeling method we have developed (Haris, Roszevák 2017).

2. HISTORICAL REVIEW

Prefabricated RC frameworks are made in many domestic and international engineering practices. Many research works have been carried out and published since the 1960s on prefabricated reinforced concrete structures and on the design of the structural details. Laboratory experiments have been performed in most study programs in the past and nowadays. Thanks to the development of computer technology, numerical studies can now be found in the literature. Although a number of scientific articles have been published on the testing of precast reinforced concrete elements, most of them involve laboratory experiments. Numerical studies on the topic can be found in very low numbers, and most of the numerical studies in the literature have been prepared by two-dimensional finite element programs; only a few research works have been completed using three-dimensional nonlinear finite element software developed specifically for reinforced concrete structures. Research programs dealing with the optimal design of RC structures and the optimization of the RC structural skeleton can also be found in the literature (Kaveh, Hosseini, Akbari 2020;

Kaveh, Hosseini, Zaerreza 2020).

In the early 1960s, prefabricated RC scarf joints were studied at the University of Illinois. In the experiments, the ultimate strength of scarf joints was found, and the behavior of the designed joints was also investigated (Gaston, Kriz 1964). Due to the proliferation of prefabricated elements, a number of attempts have been made to develop recommendations for standards for the design of elements. Prestressed and non-prestressed RC beams were investigated in the 1980s, where the torsional and shear resistance of the elements were tested (Collins, Mitchell 1980). Comparisons were made with the results of another design method, and several design examples were illustrated. From the 1980s on, more and more experimental programs were developed in seismic regions to test the resistance and behavior of prefabricated elements and the connections of prefabricated structures under cyclic loads. Pall, Marsh and Fazio (1980) developed a friction joint for large precast concrete panels, which was widely adopted throughout the world. The source of the connection problem was found in the form of the friction joint, thus the joint was designed to dissipate energy during severe seismic excitations. Already in 1977, an innovative, partially prestressed beam-column connection was investigated by Park and Thompson (1977). One of the most problematic connections for testing prefabricated frames is the column-beam connection; it was studied in several research programs (Vidjeapriya, Jaya 2013; Zhang, Ding, Rong, Yang, Wang & Zang 2020). The cyclic response of the column-beam connections was tested (Guan, Jiang, Guo & Ge 2016; Guerro, Rodriguez, Escobar, Alcocer, Bennetts & Suarez 2019). The economical design of moment resistant frame corner connections and easily constructed joints was analyzed (Choek, Lew 1991). In 2015, a two-planar, three-story frame was built and tested under vertical seismic load in Italy by Brunesi, Nascimene, Bolognini and Bellotti (2015). During the tests the inadequate seismic performance was examined and the national seismic code was synthesized. Recently, Krishnan and Purushothaman (2020) made laboratory experiments to develop a damage controllable system in the prefabricated beam-column connection by using un-bonded steel rods and cleat angles. An analytical study on a similar topic was completed by Kiss (2018). They tried to make a dissipating element in the connection and to determine the seismic performance of the developed joint. There are only few publications in the literature to examine the prefabricated column-cup foundation connection. For the examination of precast reinforced concrete, the column-to-foundation connection was tested by Tullini and Minghini (2020). They investigated the grouted duct connections of the column-pocket foundation and the positioning of the steel duct connection; and the cyclic response of the connection was analyzed in laboratory experiments.

Numerical experiments were performed on prestressed RC beam-column connections to investigate the load-bearing capacity and ductility of the joints (Ashtiani, Dhakal & Scott, 2018). The dowel connections of the precast shear wall-slab joint were analyzed in laboratory tests and numerically (3D numerical model) with ABAQUS by Arthi and Jaya (2020). Analytical studies were performed on the seismic behavior of a precast pocket foundation by Prya et al. (2016) and a three-dimensional numerical study was also made on a similar topic by Ashida and Yedhu (2017). Arthi and Jaya (2020) developed a numerical model to estimate the shear capacity of the dowel connection region. Most numerical models are exclusively 2D linear with even rarer nonlinear, and even rarer three-dimensional nonlinear finite element calculations (Hawileh, Rahman & Tabatabai, 2010).

Overall, laboratory experiments can be found in large numbers on the subject of prefabricated RC structures, however numerical studies, especially three-dimensional finite element analyses are found in small numbers in the international literature. Thus, there is definitely a reason for existence for the high-level three-dimensional nonlinear finite element analysis of prefabricated RC elements and structural connections. The differences between standard construction and design techniques are not examined, and it can be shown how much impact this has on the actual behavior of the structure.

NUMERICAL STUDY

2.1 Numerical modeling procedure

In this article we analyzed a simply prefabricated RC frame, especially the impact of connection types on the global behavior of the frame. The study was performed in the *Axis VM* (2D linear FEA) and the *ATENA 3D* (3D nonlinear FEA) software. It was examined how the prefabricated framework can be modeled in the two different software products, as well as whether the simplifications and assumptions made in the two-dimensional nonlinear finite element calculations in Axis VM are appropriate. Furthermore, in the three-dimensional nonlinear finite element software, we analyzed the individual joint designs and their modeling differences affecting the internal forces and deformations of the prefabricated RC frame. The basics of our high-level nonlinear finite element calculations in *ATENA 3D* were performed using the modeling method we developed (Haris, Roszevák 2017).

2.2 Modelling in Axis VM

For the modeling and determination of internal forces and deformations, it was necessary to create an ideal framework. The RC skeleton that was taken as a starting point has a span of 6.00 meters and a height of 4.40 meters. The column support is perfectly rigid and the column-beam joint is hinged (simply supported); see Fig.1. We defined the frame by two-dimensional finite beam elements; the end releases of the beam were hinges in the x-z plane. The static frame was defined by connecting the system line of the individual elements. The supports were assumed to be the 2/3*h (50 cm) of the cup foundation (h = height of the cup foundation). We made models for further finite element calculations where the supports were assumed at the 1/3*h (25 cm) and also the h (75 cm). The distance of the frame positions was assumed to be 5.00 m.

We reduced the vertical and the horizontal loads on the structure. The vertical loads (V_{force}) included the permanent loads (6,25 kN/m) and snow load (5,00 kN/m); they are presented in Fig. 2. The horizontal load (W_{press} and W_{suct}) was solely the wind load, in which wind suction (1.14 kN) and pressure (2.68 kN) were taken into account at the same time; see Fig. 2.

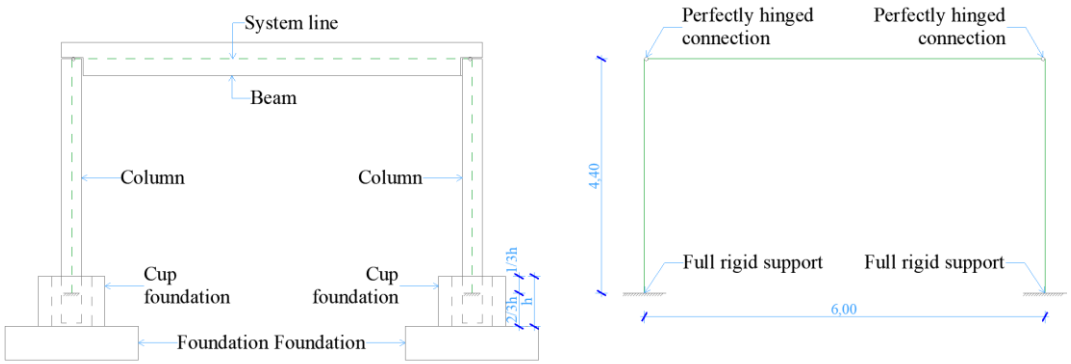

Figure 1. a The scheme of the frame; b The static frame of the RC framework (all dimensions are in m)

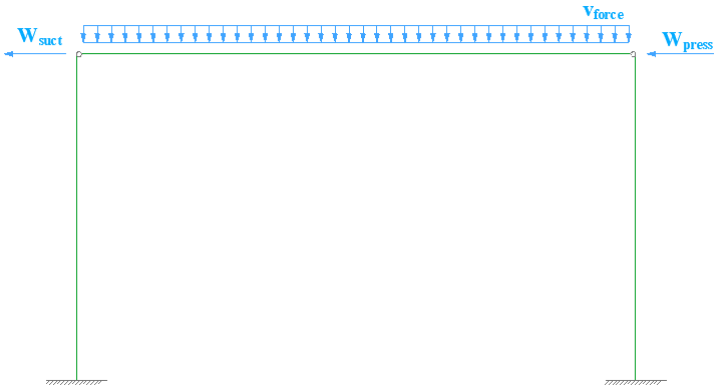

Figure 2. Loads in the model

In this model the concrete material model was linear-elastic and the calculation was nonlinear. The finite element calculations were performed for three different column and beam sizes; see Table 1.

Table 1: Details of the finite element models in Axis VM

Number of the model	Dimensions of column cross section		Dimensions of beam cross section		Strength of the concrete
	Height	Width	Height	Width	
	a [cm]	b [cm]	a' [cm]	b' [cm]	
1	30	30	50	30	C30/37
2	40	40	50	40	C30/37
3	45	45	50	45	C30/37

2.3 Modelling in ATENA 3D

The finite element models were also built up using the ATENA 3D nonlinear finite element software. In numerical studies, we analyzed, up to failure, the behavior of beam-column and column-cup foundation connections under quasi-static monotonically increasing loading. The accuracy of numerical results made by three-dimensional nonlinear finite element calculations were compared to the results of two-dimensional finite element examinations.

The geometric dimensions of the numerical models were defined also in the same way as the specimens had been analyzed in the two-dimensional finite element calculations. It was performed for two types of models: we first analyzed the column-cup foundation connection, then we investigated the frame upper joint which was the column-beam connection.

For the investigation of the foundation part, we constructed 18 different models in which the differences were in the size of the columns and the height of the filling concrete. We also built up, in the knowledge of the results, three different models to investigate:

- the shrinkage of the filling concrete,
- the column and cup surface (ribbed or flat),
- the effect of the non-perfectly rigid support.

A total of 7 ribs were placed at a height of 75 cm (height of the cup foundation and filling concrete), spaced every 10 cm. The ribs are 5 cm high, 2 cm wide and have a sloping surface of almost 45°.

We also built 30 models to examine the beam-column connection. The size of the column and the shape of the beam was analyzed and we also investigated:

- the behavior of the number of the dowels in the connection,
- the filling concrete strength around the dowels,
- the size of the neoprene sheet between the column and the beam,
- the placement inaccuracy of the dowels.

The defined formations and the connection parameters are summarized in Table 2 and Table 3; for the symbols given in the tables see Fig. 3.

Table 2: Details of the finite element models in ATENA 3D – column-cup foundation models

	Size of the column	Size of the cup foundation		Size of the filling concrete		Strength of the concrete	Strength of the filling concrete
	h x b [cm]	v' [cm]	h' x b' x m' [cm]	v [cm]	m' [cm]		
O30-KM75-KA25	*30 x 30*	*20*	*100 x 100 x 75*	*15*	*75*	*C30/37*	*C25/30*
O40-KM75-KA25	*40 x 40*	*20*	*100 x 100 x 75*	*10*	*75*	*C30/37*	*C25/30*
O45-KM75-KA25	*45 x 45*	*20*	*105 x 105 x 75*	*10*	*75*	*C30/37*	*C25/30*
O30-KM50-KA25	*30 x 30*	*20*	*100 x 100 x 75*	*15*	*50*	*C30/37*	*C25/30*
O40-KM50-KA25	*40 x 40*	*20*	*100 x 100 x 75*	*10*	*50*	*C30/37*	*C25/30*
O45-KM50-KA25	*45 x 45*	*20*	*105 x 105 x 75*	*10*	*50*	*C30/37*	*C25/30*
O30-KM25-KA25	*30 x 30*	*20*	*100 x 100 x 75*	*15*	*25*	*C30/37*	*C25/30*
O40-KM25-KA25	*40 x 40*	*20*	*100 x 100 x 75*	*10*	*25*	*C30/37*	*C25/30*
O45-KM25-KA25	*45 x 45*	*20*	*105 x 105 x 75*	*10*	*25*	*C30/37*	*C25/30*
O30-KM75-KA20	*30 x 30*	*20*	*100 x 100 x 75*	*15*	*75*	*C30/37*	*C20/25*
O40-KM75-KA20	*40 x 40*	*20*	*100 x 100 x 75*	*10*	*75*	*C30/37*	*C20/25*

O45-KM75-KA20	*45 x 45*	*20*	*105 x 105 x 75*	*10*	*75*	*C30/37*	*C20/25*
O30-KM50-KA20	*30 x 30*	*20*	*100 x 100 x 75*	*15*	*50*	*C30/37*	*C20/25*
O40-KM50-KA20	*40 x 40*	*20*	*100 x 100 x 75*	*10*	*50*	*C30/37*	*C20/25*
O45-KM50-KA20	*45 x 45*	*20*	*105 x 105 x 75*	*10*	*50*	*C30/37*	*C20/25*
O30-KM25-KA20	*30 x 30*	*20*	*100 x 100 x 75*	*15*	*25*	*C30/37*	*C20/25*
O40-KM25-KA20	*40 x 40*	*20*	*100 x 100 x 75*	*10*	*25*	*C30/37*	*C20/25*
O45-KM25-KA20	*45 x 45*	*20*	*105 x 105 x 75*	*10*	*25*	*C30/37*	*C20/25*

Table 3: Details of the finite element models in ATENA 3D – beam-column models

Model number	Size of the column		Size of the beam		Diameter of the dowel [mm]	Number of the dowels		Position of the dowel	Strength of filling concrete	Width of the neoprene sheet c [cm]	Direction of the horizontal load
	h [cm]	b [cm]	h* [cm]	b* [cm]		x direction	y direction				
1	*30*	*30*	*50*	*30*	*25*	*1*	*1*	*middle*	***Sikagrout***	*10*	*positive*
2	*30*	*30*	*50*	*30*	*25*	*1*	*1*	*middle*	*C40/50*	*10*	*positive*
3	*30*	*30*	*50*	*30*	*25*	*1*	*1*	*middle*	***C45/55***	*10*	*positive*
4	*30*	*30*	*50*	*30*	*25*	*1*	*1*	*middle*	***C50/60***	*10*	*positive*
5	*30*	*30*	*50*	*30*	*25*	*1*	*1*	*middle*	***C60/75***	*10*	*positive*
6	***40***	***40***	*50*	***40***	*25*	*1*	*1*	*middle*	*C40/50*	*10*	*positive*
7	***45***	***45***	*50*	***45***	*25*	*1*	*1*	*middle*	*C40/50*	*10*	*positive*
8	*30*	*30*	*50*	*30*	***20***	*1*	*1*	*middle*	*C40/50*	*10*	*positive*
9	*30*	*30*	*50*	*30*	***16***	*1*	*1*	*middle*	*C40/50*	*10*	*positive*
10	*30*	*30*	*50*	*30*	*25*	***2***	***1***	*middle*	*C40/50*	*10*	*positive*
11	*30*	*30*	*50*	*30*	*25*	***1***	***2***	*middle*	*C40/50*	*10*	*positive*
12	*30*	*30*	*50*	*30*	*25*	***2***	***2***	*middle*	*C40/50*	*10*	*positive*
13	*30*	*30*	*50*	*30*	*25*	***1***	***1***	***negative x***	*C40/50*	*10*	*positive*
14	*30*	*30*	*50*	*30*	*25*	***2***	***1***	***negative x***	*C40/50*	*10*	*positive*
15	*30*	*30*	*50*	*30*	*25*	***1***	***2***	***negative x***	*C40/50*	*10*	*positive*
16	*30*	*30*	*50*	*30*	*25*	***2***	***2***	***negative x***	*C40/50*	*10*	*positive*
17	*30*	*30*	*50*	*30*	*25*	***1***	***1***	***positive x***	*C40/50*	*10*	*positive*
18	*30*	*30*	*50*	*30*	*25*	***2***	***1***	***positive x***	*C40/50*	*10*	*positive*
19	*30*	*30*	*50*	*30*	*25*	***1***	***2***	***positive x***	*C40/50*	*10*	*positive*
20	*30*	*30*	*50*	*30*	*25*	***2***	***2***	***positive x***	*C40/50*	*10*	*positive*
21	*30*	*30*	*50*	*30*	*25*	*1*	*1*	*middle*	*C40/50*	***12***	*positive*
22	*30*	*30*	*50*	*30*	*25*	*1*	*1*	*middle*	*C40/50*	***14***	*positive*
23	*30*	*30*	*50*	*30*	*25*	*1*	*1*	*middle*	*C40/50*	***16***	*positive*
24	*30*	*30*	*50*	*30*	*25*	*1*	*1*	*middle*	*C40/50*	***18***	*positive*
25	*30*	*30*	*50*	*30*	*25*	*1*	*1*	*middle*	*C40/50*	***20***	*positive*
26	*30*	*30*	*50*	*30*	*25*	*1*	*1*	*middle*	*C40/50*	*10*	***negative***
27	*30*	*30*	*50*	*30*	*25*	***1***	***1***	***negative x***	*C40/50*	*10*	*positive*
28	*30*	*30*	*50*	*30*	*25*	***1***	***1***	***positive x***	*C40/50*	*10*	*positive*
29	*30*	*30*	***Notched***		*25*	***1***	***2***	*middle*	*C40/50*	*10*	*positive*
30	***40***	***40***	***Notched "T"***		*25*	***1***	***2***	*middle*	*C40/50*	*10*	*positive*
31	***40***	***40***	***"T" cross section***		*25*	***1***	***2***	*middle*	*C40/50*	*10*	*positive*
32	***Full model***				*25*	***1***	***2***	*middle*	*C40/50*	*10*	*positive*

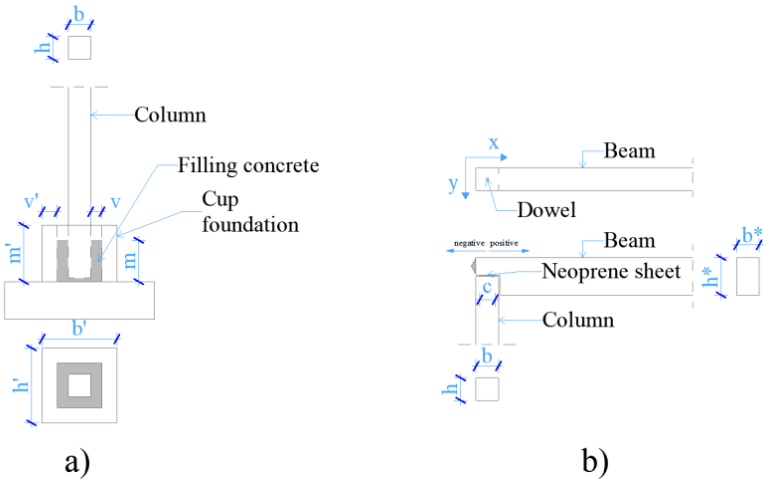

Figure 3 Parameters of the joints a Column-cup joint; b Beam-column joint

Basically, we made separate joint models of the prefabricated frame; however, using the results of the joint models, we also created a complex frame model. The built-up models are illustrated in Fig. 4. See Fig. 5 for the reinforcement parameters of the column-beam joint. The reinforcement parameters of the column-pocket foundation models are given in Fig. 6. The column-beam joint was examined with four different dowel settings; see Fig. 7.

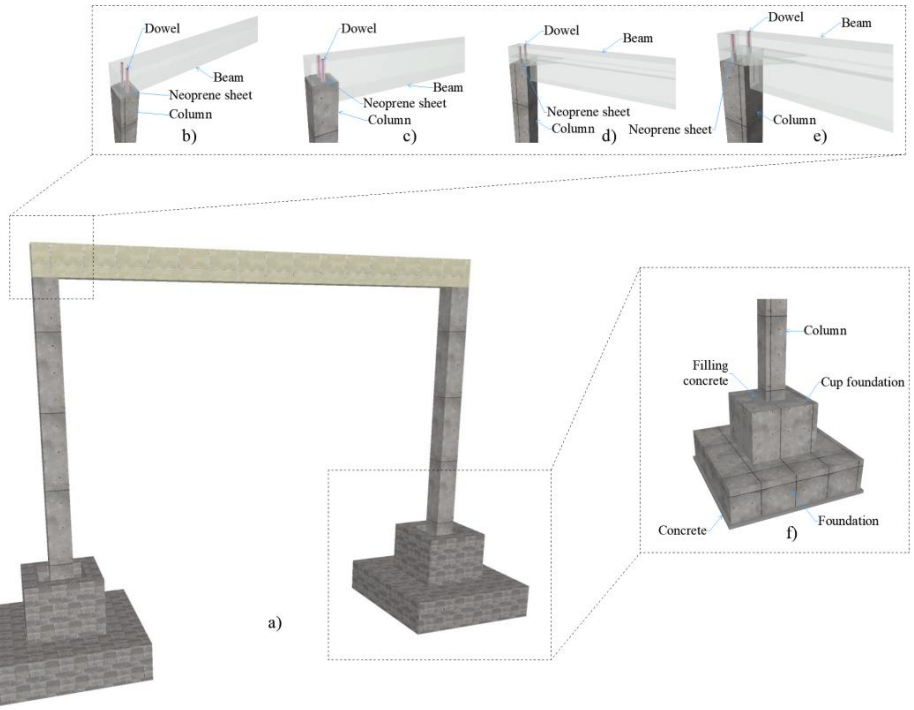

Figure 4. Schemes of the frame a Global model; b Straight-ended beam; c Notched-ended beam; d "T" cross section with notched end; e "T" cross section with "pocket" end; f cup foundation-column connection

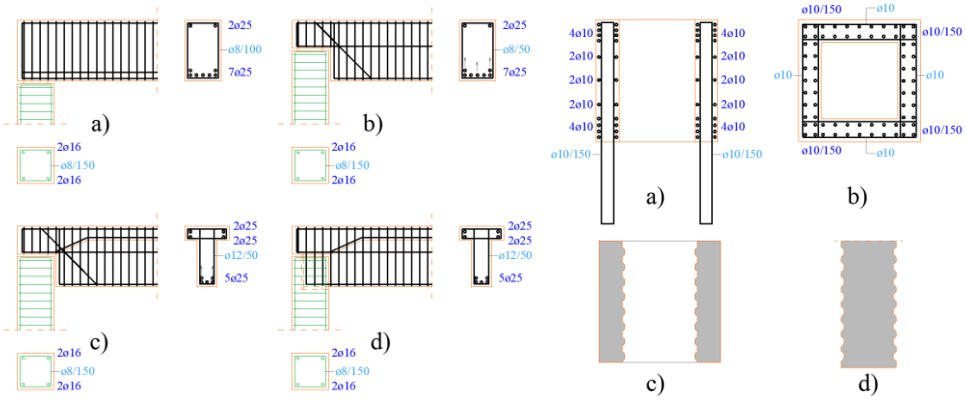

Figure 5. Different types of the beam-column joints
a Straight beam; b Notched end beam;
c "T" cross section with notched end
d "T" cross section with "pocket" end

Fig. 6 The scheme of the column-cup joints
a horizontal reinforcement;
b vertical reinforcement
c ribbed cup; d ribbed column

For the joint models, the loads acting on the entire frame were reduced. For the beam-column model, the vertical load (V [kN/m^2]) on the beam was defined in 10 load steps. In the column-pocket foundation model, the vertical load (V [kN]) was also placed in 10 load steps at the top of the column. In both models, the horizontal load was modeled by a concentrated displacement load (e [mm]). For the loads specified for the models see Fig 8. We placed a monitor point at the point of the displacement load where the generated force was detected.

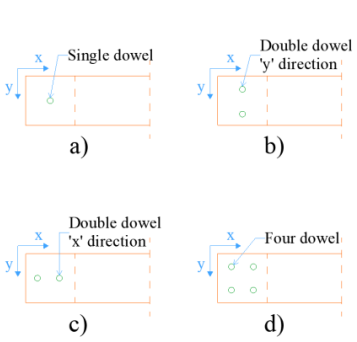

Figure 7. Position of the dowels
a single dowel; b double dowel 'y' direction
c double dowel 'x' direction; d four dowels

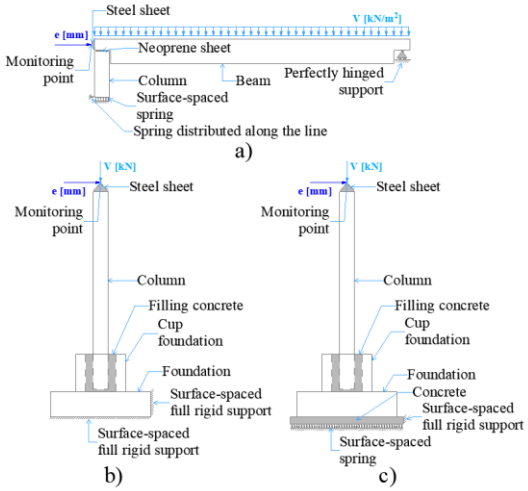

Fig. 8 Loading layout
a beam-column model; b column-cup model
c modeling of the non-perfectly rigid support

In the numerical experiments, the material model of concrete was defined with an individually parametrized model on the basis of our previous results (Haris, Roszevák 2017). The concrete material model includes the following effects of concrete behavior

(Cervenka et al. 2014): non-linear behaviour in compression including hardening and softening, reduction of compressive strength after cracking (Van Mier 1986), fracture of concrete in tension based on nonlinear fracture mechanics (Hordijk 1991), biaxial strength failure criterion (Kupfer et al. 1969), tension stiffening effect, reduction of shear stiffness after cracking (Kolmar, 1986), and the fixed (Cervenka 1985, Darwin, Pecknold 1974) and rotated (Vecchio, Collins 1986, Crisfield, Wills, 1989) crack direction. The reinforcement material model is specified according to the properties of the reinforcement, the real stress-deformation characteristics are provided. The strength properties of the concrete and reinforcement bars, and the other material parameters were defined based on (Roszevák, Haris 2019). The concrete strength in case of the beam, the column and the pocket foundation were C30/37, and the reinforcement and the dowel were defined according to S500B. The relationship between concrete and reinforcement bars was calculated and defined based on the CEB-FIB Model Code 1990 (CEB-FIB model code 1990). The longitudinal bars were modeled with their real geometry and diameter, the stirrups with a closed rectangular shape other than the actual bending shape, but with their real diameter.

For all nonlinear analyses, an iterative method (Newton-Raphson iteration method) was used to perform the iteration process. The Cholesky resolution was used to solve the state equation of the structure. In numerical models we used uniformly quadratic bar functions, and we used 20-node brick (in case of the column and beam) and 10-node tetra (in case of cup foundation and on the beam ends) elements for the concrete (Roszevák, Haris 2019; Haris, Roszevák 2017); see Fig 9. The finite element mesh is distributed uniformly so that there are at least 4 finite elements within the given cross-sectional dimension (Haris, Roszevák, 2017). This means in our models that the size of the finite element mesh surrounding the joint is not bigger than 4-5 cm. The basic mesh size of the other part of the model was 10-15 cm. It should be noted that a denser mesh was used in the vicinity of the joints for the ribbed column design and the beam-column joint. The filling concrete, the dowel and the neoprene sheet were constructed of a body element which was also defined by tetra elements. The material model for the neoprene sheet was parametrized based on previous research (Hooper 1964; Fediuc, Budescu, Feduic, Venghiac 2013).

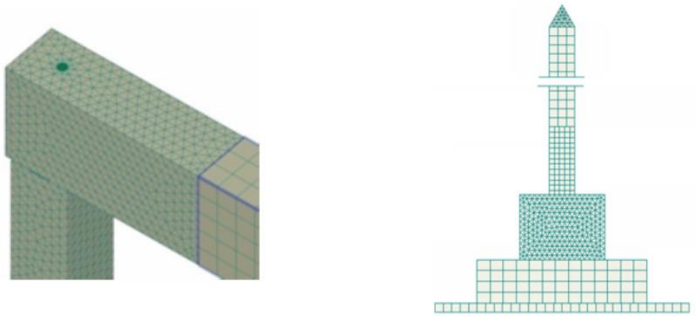

a) b)

Figure 9. Mesh on finite element models a beam-column model; b column-cup foundation model

In this research, a new contact element also had to be defined, which was placed between the concrete-concrete, the concrete-neoprene sheet and the concrete-dowel elements. The

contact element can only absorb pressure and compression due to the roughness of the surface of the elements. In order for the numerical calculation to be performed, the tensile parameter of the contact element had to be given a value very close to zero.

3. NUMERICAL INVESTIGATION OF THE POCKET FOUNDATION

The studies were started with the Axis VM software, where the results obtained by linear calculations are plotted on a force-top displacement graph. The resulting horizontal forces in the Axis VM were applied to the ATENA 3D model. The results are shown in a common graph; see Fig. 10.

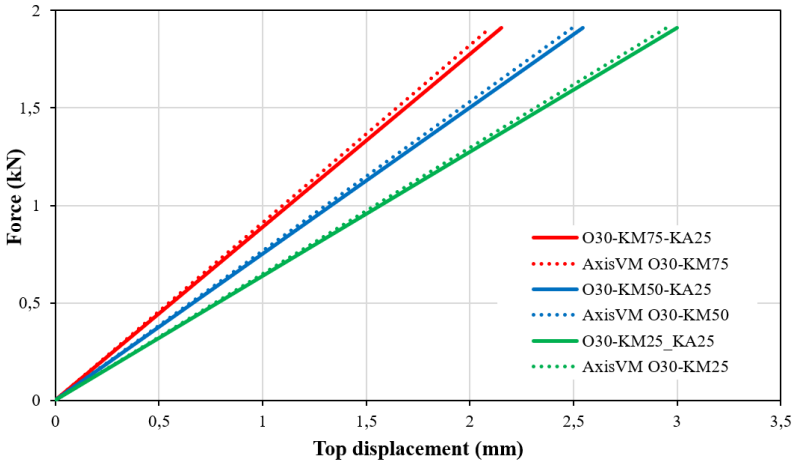

Figure 10. Force-displacement diagram – in case of 30*30 cm column size

Table 4: Comparison of the results in case of 30*30 cm column size

Modell	Force	AxisVM non-linear	Atena3D non-linear	Difference [%]
		Horizontal top displacement [mm]	Horizontal top displacement [mm]	
O30-KM75-KA25	1.91	2.098	2.151	2.46
O30-KM50-KA25	1.91	2.493	2.546	2.08
O30-KM25-KA25	1.91	2.948	2.999	1.70

Based on the results, it can be stated that the height of the filling concrete (which was different between the three ATENA 3D models) has a significant effect on the magnitude of the horizontal load. Numerically, a reduction of ~ 28.27 % is caused by the decrease in the height of the filling concrete. At the same load level (1.91 kN), there is a difference of almost 1.70-2.46 % between the Axis VM and the Atena 3D models.

After the first 18 numerical runs, a load equal to the relative horizontal displacement limit (e = 30 mm) was defined for each model. The force-displacement diagrams of the calculations performed in this way are provided in Fig. 11, according to the column cross-

section. The curves of the models with different filling heights are well separated from each other, in contrast to the curves of the models with different filling material qualities, where only minimal differences can be observed.

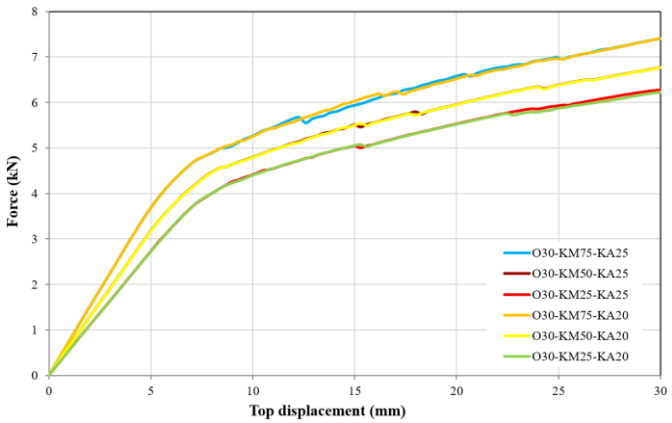

a)

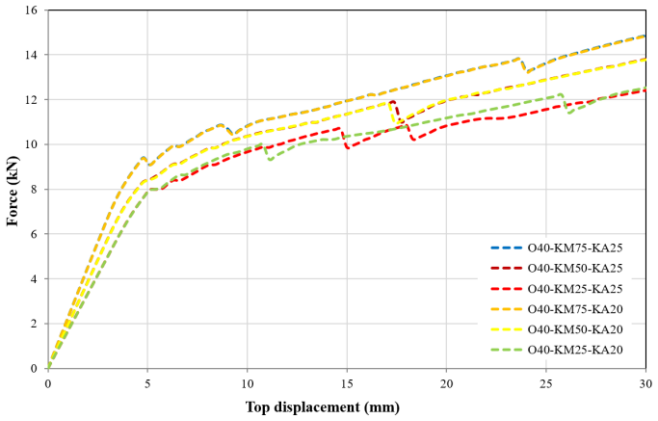

b)

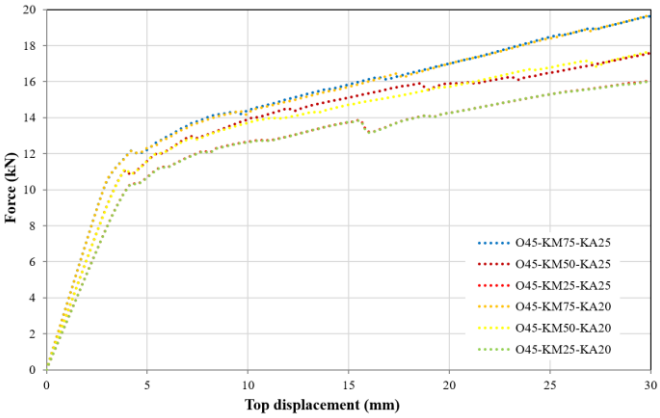

c)

Figure 11. Load-displacement diagrams – in case of different filling concrete strength a O30 models; b O40 models; c O45 models

Table 5: Values of horizontal forces in case of 30 mm displacement loading

Model	KM75		KM50		KM25	
	KA20	KA25	KA20	KA25	KA20	KA25
O30	7.63 kN	7.63 kN	6.97 kN	6.97 kN	6.42 kN	6.45 kN
O40	15.44 kN	15.45 kN	13.90 kN	13.92 kN	12.68 kN	12.83 kN
O45	20.40 kN	20.40 kN	18.25 kN	18.39 kN	16.45 kN	16.46 kN

The results show that the change in the material quality of the filling concrete does not have a significant effect on the horizontal force at the monitoring point of the models: the largest difference is ~ 1% for the O40-KM25 models; see Table 5. In contrast, for all three column sizes, it can be observed that as the height of the filling concrete decreases, the horizontal reaction force also decreases by nearly 15-19% (between the KM75 and KM25 models).

After loading the 18 models with the horizontal displacement limit, we performed another run on each with higher horizontal displacement values. The reason for this was to examine the behavior of the joints even in the case of large deformations compared to the structural system. When evaluating the results, it can be established that the model properly follows the behavior characteristic of this type of structures. It has been observed from previous analyses that changes in the material quality of the filling concrete do not significantly affect the development of the results. In this section, the results of the first 9 models (where the filling concrete is C25 / 30 material quality) are described and compared. The comparison is again performed on the basis of force-displacement diagrams, similar to the previous ones, also grouped by column size (Fig. 12). Looking at the results, the values of the peak force present different values for each column cross-section, which were 12.19 kN (30 * 30 cm), 19.41 kN (40 * 40 cm) and 22.94 kN (45 * 45 cm) for the 75 cm filling concrete height. The same tendency can be observed in the case of models tested with lower heights of filling concrete.

Depending on the height of the filling concrete, the peak force associated with the highest and lowest filling concrete (12.19 kN-10.54 kN; 19.42 kN-17.12 kN; 22.94 kN-20.62 kN) show a difference of nearly 10-14 %. With regard to the displacements associated with peak force, the results are already significantly different, ranging from 16% to 32%, depending on the filling concretes of different heights and the cross-sections of the column.

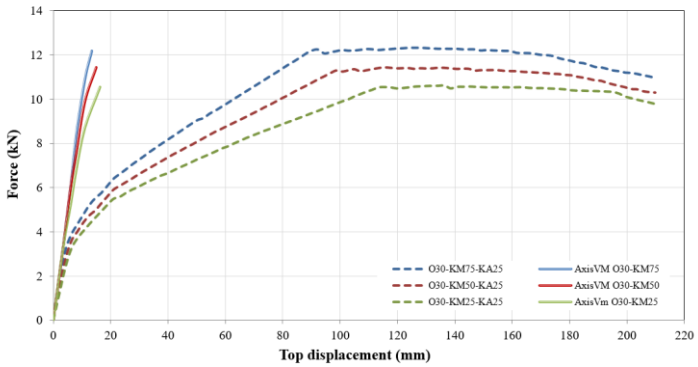

a)

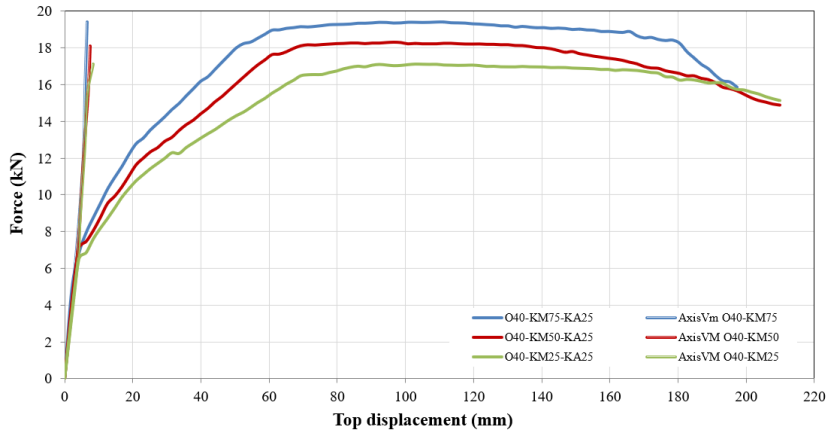

b)

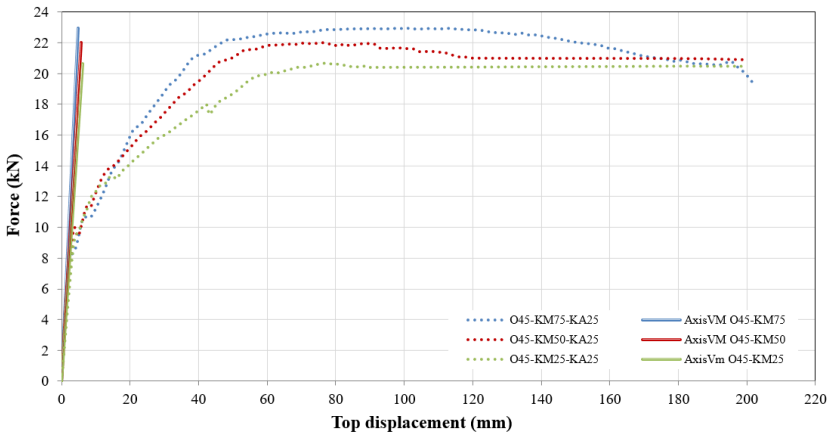

c)

Figure 12. Load-displacement diagrams in case of different column sizes
a O30 models; b O40 models; c O45 models

Table 6: Comparison of the results – different column sizes

	Model	Peak force [kN]	Top displacement [mm]
	KM75-KA25	***12.196***	*90.30*
O30-	KM50-KA25	*11.437*	*117.60*
	KM25-KA25	*10.542*	*132.30*
	KM75-KA25	***19.416***	***115.50***
O40-	KM50-KA25	*18.125*	*98.70*
	KM25-KA25	*17.117*	*96.60*
	KM75-KA25	***22.937***	***98.70***
O45-	KM50-KA25	*22.009*	*76.80*
	KM25-KA25	*20.623*	*74.30*

Based on Table 6, it can be concluded that the height of the infill concrete has a

significant effect on structural behavior. We analyzed the difference between the AxisVM and ATENA 3D models, where there is a significant difference in terms of displacements by the same force (peak force). The displacements in the AxisVM models are orders of magnitude smaller than the ATENA 3D models, so they cannot be compared either; see Fig. 12. Based on the results obtained with the created models, it will be possible to analyze the energy dissipated by the structure in a later research program. Furthermore, based on the results obtained, it can be stated that the height of the filling concrete formed during construction can have a significant effect on the behavior of the structure, so it must / can be duly taken into account during the design of the structure.

In the joint we modeled, the gap between the prefabricated column and the cup foundation is filled with cast-in-situ infill concrete. The filling concrete shrinks during solidification, so we considered it important to model its effects on the structure. Shrinkage was modeled in three ways during our investigations. First, a shrinkage deformation was parameterized, then the shrinkage deformation was replaced by a temperature load, and finally the tensile strength of the filling concrete was reduced. The shrinkage load was applied to the "O30-KM75-KA25" model and then compared with the results of the original model. In the model, this value of ε_0 was defined for a built-in shrinkage load on the filling concrete. The "load" of shrinkage was given in one loading step before the quasi-static vertical load and the horizontal displacement load.

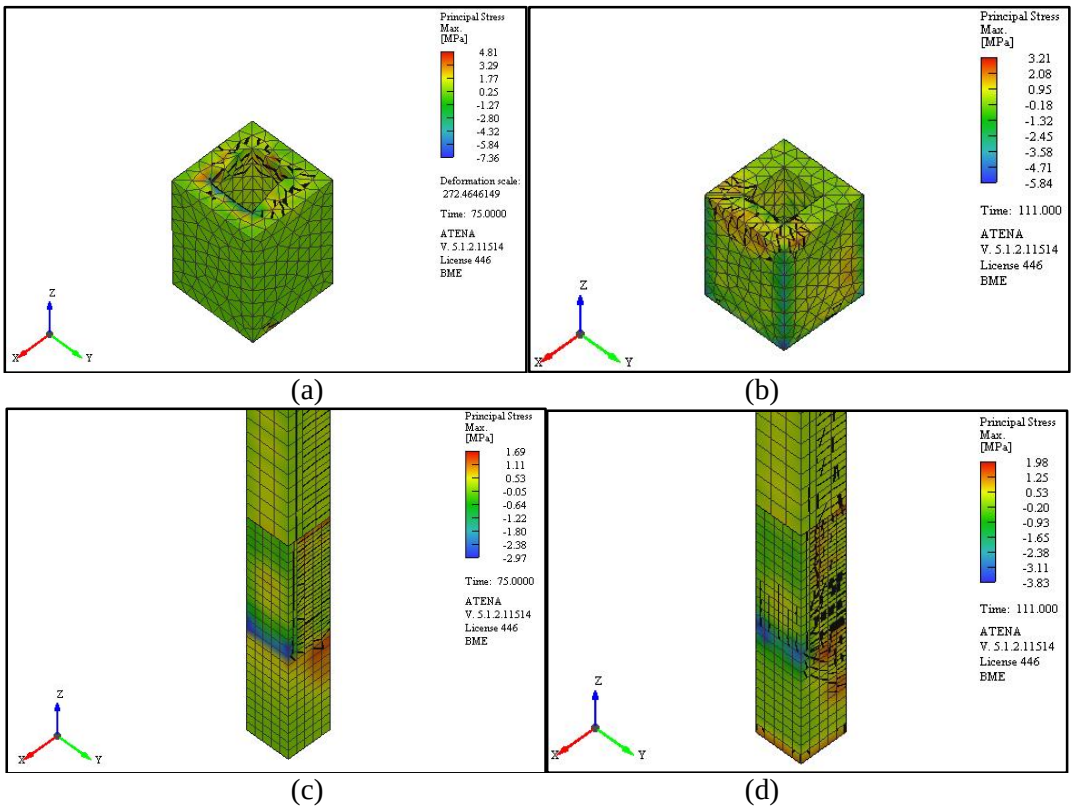

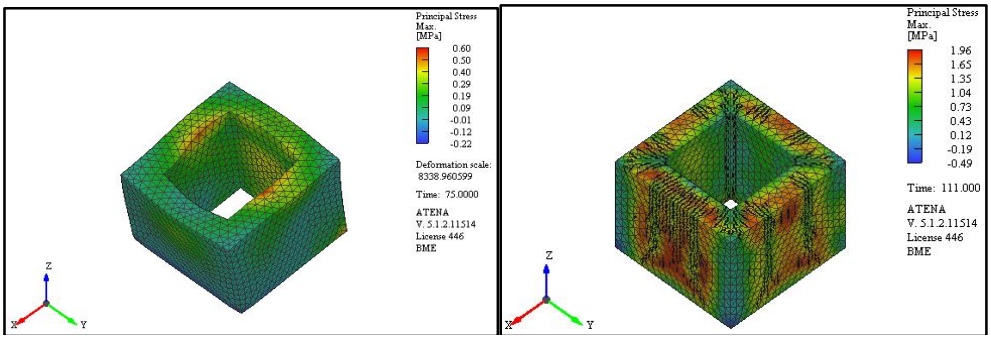

(e) (f)

Figure 13. Stress figures on filling concrete [a without shrinkage; b with shrinkage], column [c without shrinkage; d with shrinkage] and cup foundation [e without shrinkage; f with shrinkage]

The results show that shrinkage modeling with shrinkage deformation affects the global behavior of the structure. Failure occurs at nearly equal horizontal force levels (with shrinkage: 12.02 kN; without shrinkage: 12.23 kN), but the displacement associated with these values increases by nearly 6.09% (with shrinkage: 98.40 mm; without shrinkage: 92.40 mm). If we examine the structural elements locally, it can be observed that the stresses of the filling concrete decrease (~ 20-30%), while the stresses of the pillar and cup foundation increase (~ 15-70%) as a result of shrinkage. For shrinkage modeled with reduced the tensile strength, the results for the force of failure (3.13 kN / 3.13 kN) and the associated displacement (4.20 mm / 4.20 mm) are the same for the original model and the reduced tensile strength model. However, the values for force of failure (12.23 kN / 12.17 kN) and displacement (92.40 mm / 91.20 mm) differ by 0.49% (force) and 1.29% (displacement). If we examine the structural elements locally, it can be observed that the stresses of the filling concrete decrease (~ 20%), while the stresses of the pillar and cup foundation increase (~ 10-20%) as a result of shrinkage. For changes in the stresses in the filling concrete, column, and cup foundation as a result of shrinkage, see Fig. 13; the change in the force-displacement diagram is shown in Fig. 14.

The temperature load substituting for shrinkage was calculated from the final value of the shrinkage deformation. In the “O30-KM75-KA25” model; a substitute temperature load was applied to the filling concrete element, the value of which was 30.2 K.

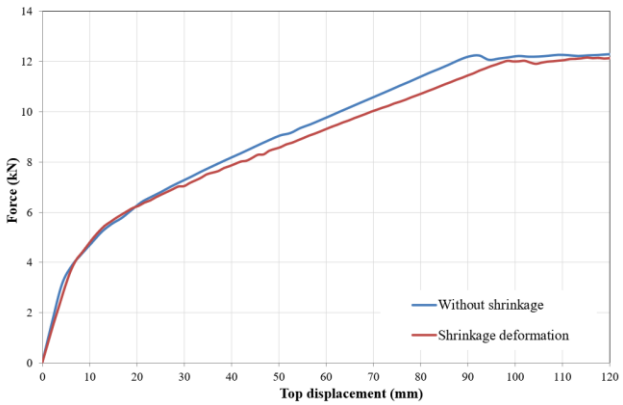

Figure 14. Load-displacement diagrams – in case of modeling the shrinkage on “O30-KM75-KA25” model

Table 7: Comparison of the results – in case of modeling the shrinkage on "O30-KM75-KA25" model

O30-KM75-KA25	Peak force [kN]	Top displacement [mm]
Without shrinkage	12.23	92.40
Shrinkage deformation	12.02	98.40

The outer vertical surfaces of the prefabricated columns and the inner vertical surfaces of the prefabricated cup foundations are generally ribbed in order to increase the size of the cooperating surfaces in contact with the infill concrete and to improve the rigid connection. With this form, the column and the cup foundation cooperation can be significantly increased. In the "O45-KM75-KA25" model we created a real rib (https://ferrobeton.hu/images/upload/content/1498/files/KEHS.pdf), both at the bottom of the column and at the inside of the cup foundation. The results of the numerical calculations performed in this way were compared with the results of the original model "O45-KM75-KA25". The change in the force-displacement diagram is shown in Fig. 15, and the change in the stresses of the column, the filling concrete, and the cup foundation as a result of ribbing is shown in Fig. 16.

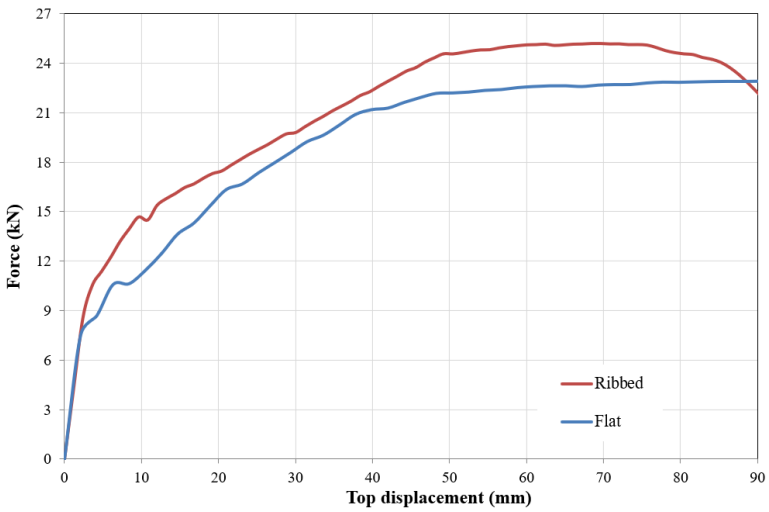

Figure 15. Load-displacement diagrams – in case of modeling the column with ribbed and flat surface

Table 8: Comparison of the results – in case of modeling the column with ribbed and flat surface

O45-KM75-KA25	Peak force [kN]	Top displacement [mm]
Flat column and cup	22.18	48.30
Ribbed column and cup	24.56	49.20

The models with the ribbed surface of the cup foundation and the force-displacement diagram of the original model have nearly the same characteristics; however, by examining the peak force, the model with the ribbed cup is able to absorb more force. In examining the peak force, we already see larger differences. In the ribbed case, the force of failure is 24.56

kN, and in the case of a flat cup, it is 22.18 kN. There was no significant difference in displacements by peak force, between 49.20 mm (ribbed) and 48.30 mm (flat). In examining the peak force, the ribbed model is able to absorb nearly 10% more force, with deformations increasing by only 1.8 % compared to the results obtained using models of cup foundation modeled with a flat inner surface. In terms of global frame, the ribbed design has an effect on the load capacity of the structure. If we examine the structural elements locally, it can be observed that the effect of ribbing increases both tensile (4.36 MPa-8.10 MPa) and compressive stresses (-3.00 MPa-30, 56 MPa).

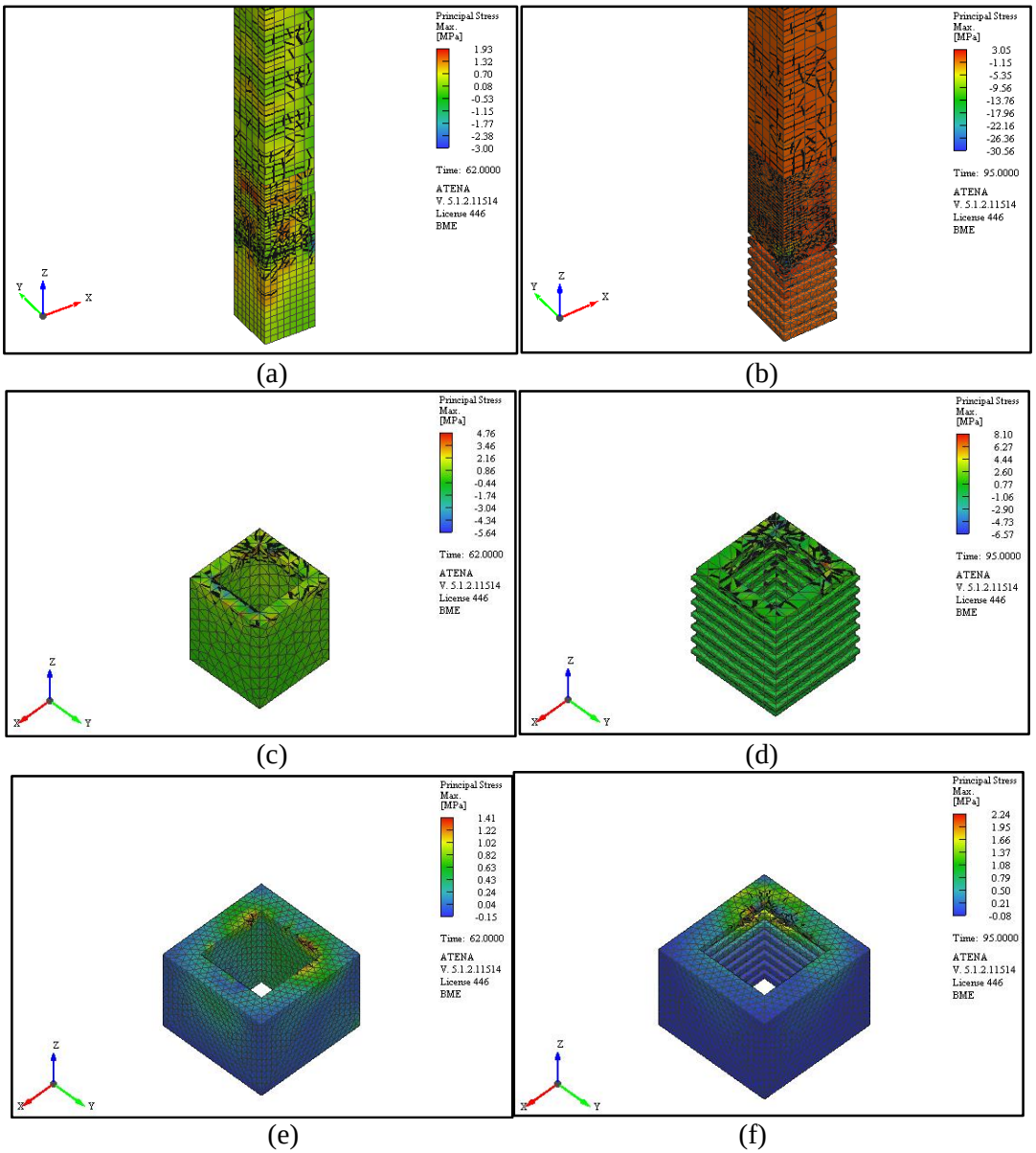

Figure 16. Stress figures on column [a smooth; b ribbed], filling concrete [c smooth; d ribbed] and cup foundation [e smooth; f ribbed]

The foundation was prepared with soil parameters typical in Hungary. Based on our investigations, the supporting effect of the soil can be modeled; however, the models that take into account the actual soil stratification can be examined in further research programs. The same calculation as before was performed in this case as well. The force-displacement diagrams are shown in Fig. 17.

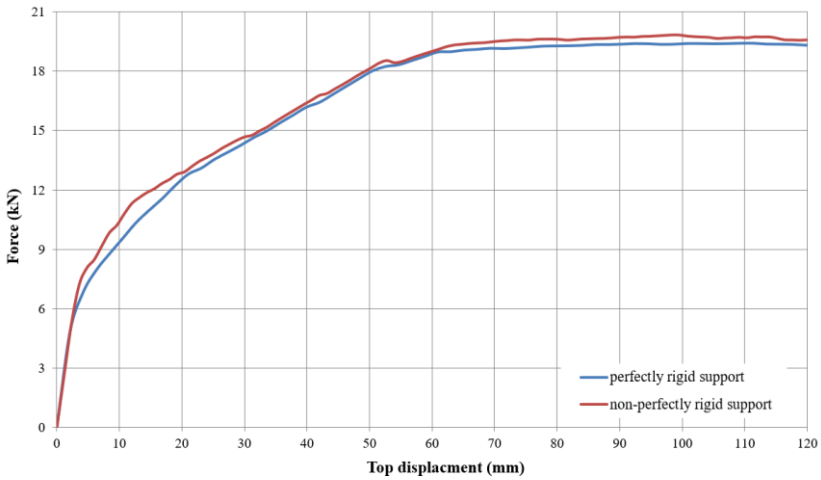

Figure 17. Force-top displacement diagrams – in case of modeling the non-perfectly rigid support

4. NUMERICAL INVESTIGATION OF THE BEAM-COLUMN JOINT

In the next step, we examined the column-beam connection in an independent model. The deflection of a simple frame beam was investigated with the Axis VM program; see Fig. 12. Vertical loads were placed on the simple supported beam and the same load was placed in the ATENA 3D on the separate column-beam model.

Figure 18. Load in the model

As a result of the vertical load, a stress distribution corresponding to the bending was created in both the beam and the reinforcing bars placed in it for all numerical models. The beam is also cracked in the tensile zone; see Fig. 19. In the case of a linear calculation, the value of the bending moment generated in the beam is 57.5 kNm under the influence of vertical loads. In determining the value of the extreme fiber stress, the value of 5.70 MPa was obtained, which exceeds the characteristic value of the tensile strength of the concrete taken into account in the models, so the tensile zone cracked (as in the case of non-linear models). In this case we only investigated the the load value up to 18 kN, so the deflections are made with this load value. The results from the ATENA 3D and the Axis VM calculations are shown on a vertical load-deflection diagram; see Fig. 20.

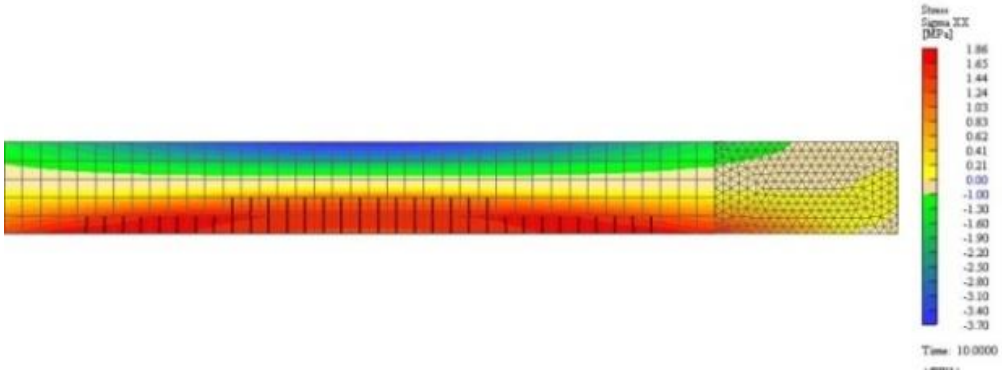

Figure 19. Stress distribution and crack pattern in the beam at the 10. load step

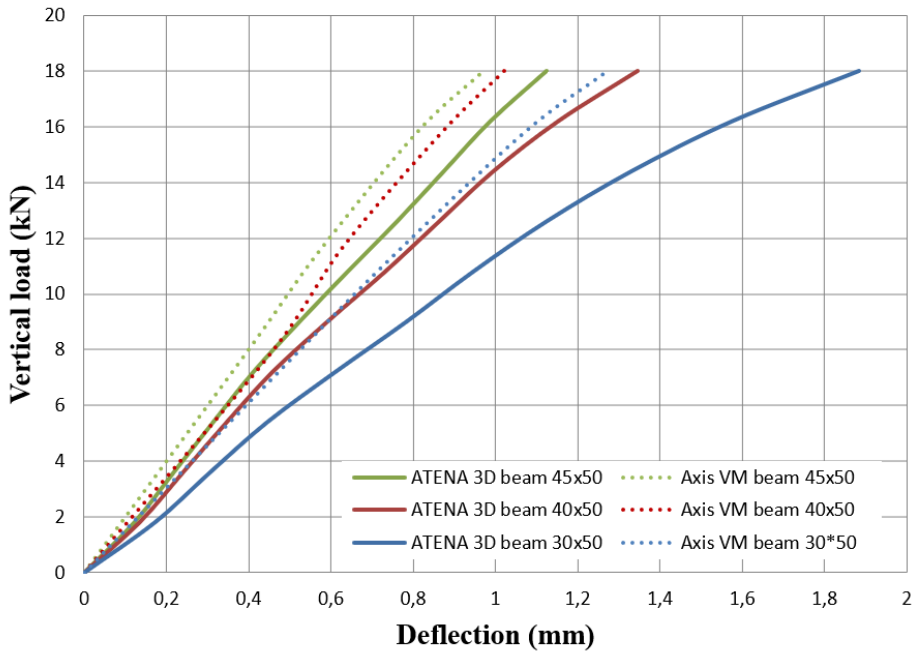

Figure 20. Vertical load-deflection diagrams – in case of different beam cross sections

Table 9: Deflections in the middle of the beam in case of rectengular beam cross section

Model/beam cross section	Axis VM Deflection [mm]	ATENA 3D Deflection [mm]	Difference [%]
30*50	1.275	1.883	32.28
40*50	1.027	1.345	23.64
45*50	0.971	1.125	13.68

Based on Table 9, we can state that the beam deflections were significantly underestimated by the simple finite element calculations. The deflections obtained in the Axis VM exceed nearly 32 % in the case of the 30*50 beam cross section.

In the next step we analyzed the end form of the beam. In addition, similarly to the column end form, we also examined the deflections of the middle point of the beam. In this case we only described the 30*50 beam cross-section; see Fig. 24. The deflection belonging to 18 kN load value developed similarly to the previous investigations. The deflections belonging to Axis VM are 32.28 % (ATENA 3D straight beam) and 47.93 % (ATENA 3D notched ended beam) smaller; see Table 9.

Overall, we can say that the depth of the computational technique and the form of the beam end greatly influence the deformations of the beam. We found a very large difference between the different finite element processes in terms of beam deflection. In all cases, the deflection value obtained in the linear calculation was the smallest, which is trivially due to the difference between the two calculation methods.

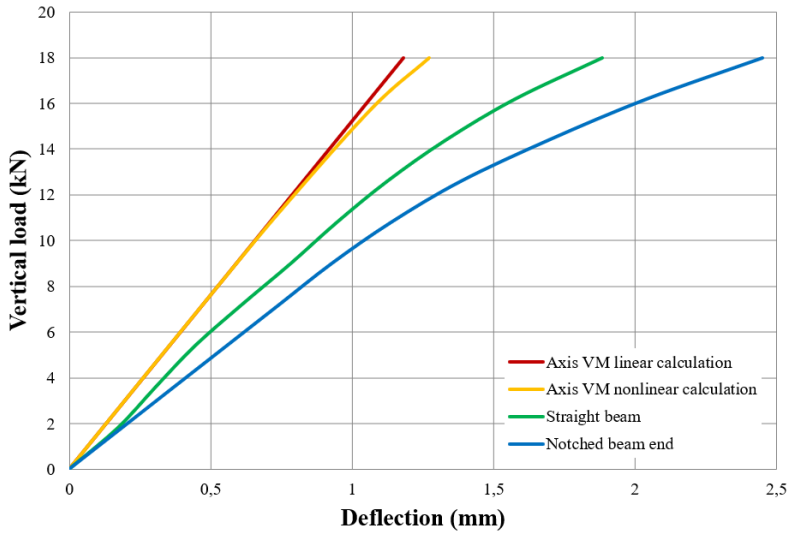

Figure 21. Vertical load-deflection diagrams – in case of different beam end form

Table 9: Deflections in the middle of the beam in case of different beam end forms

Model	Axis VM linear Deflection [mm]	Axis VM nonlinear Deflection [mm]	ATENA 3D straight Deflection [mm]	ATENA 3D notched ended Deflection [mm]
30*50	1.182	1.275	1.883	2.449

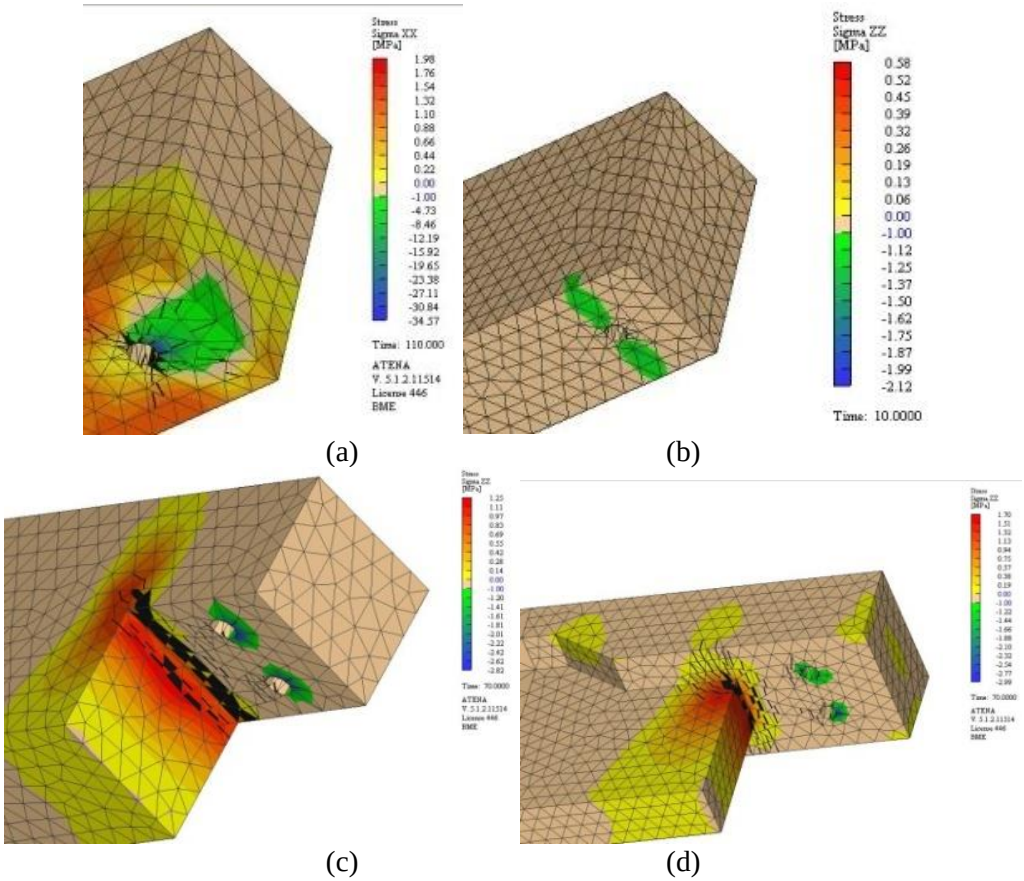

Figure 21. Stress distribution in the beam in the vicinity of the dowels a stress 'XX' in the 110. load step; b stress 'ZZ' in the 10. load step; c stress 'ZZ' on notched end beam in the 70. load step; d stress 'ZZ' on notched end 'T' shape beam in the 70. load step

The end form of the beam also generates a special stress distribution: in case of the notched-end beam, a stress peak develops in the notch; see Fig. 21. In the case of models with a notched end, despite the amount of reinforced concrete placed in the beams, cracks and vertical stress peaks occur in the concrete in the vicinity of the notch. In the pocket design, unlike the beams with the notched support end, no cracks or stress peaks formed in the vicinity of the connection; see Fig. 21.

In the next step we described the results for dowels and their effect on the behavior of the structure. As expected, and specified in the standards, shear and bending were also generated in the dowels based on the results obtained in the numerical models; however, the stresses resulting from shear were in each case lower than the values resulting from bending. In the further phase of the load, horizontal (global x-direction) stress peaks (maximum compressive stress 34.57 MPa) and cracks developed in the vicinity of the dowel for all geometric designs. The extreme values of the stresses in the dowels are shown in Table 10 below.

Table 10: Values of the stresses in the dowels

Diameter [mm]	Load step	Stress from shear [MPa]	Stress from bending [MPa]	Compression stress from bending [MPa]
25	70	67	186	180
	110	220	554	680
20	70	67	191	202
	110	217	536	572
16	70	111	300	310
	110	211	536	559

The dowel has entered a plastic state by the end of the experiment for all diameters (yield strength in the defined material model: f_y = 500 MPa), while at a horizontal displacement of 3.00 cm (load step 70) the tendency of the extreme values of the bending stresses is inversely proportional to the diameter of the dowel. At the end of the test this is no longer satisfied before the shear stress reached the yield point of the defined material model. The use of more dowels did not change the values of the principal stresses in the dowels. The test was displacement-controlled in all cases, the force-displacement diagram measured at the apex of the load plate was affected by a change in the number of pieces used and the geometric placement.

Table 11: Deflections in the middle of the beam in case of rectengular beam cross section

Number of dowels in plane of the frame	Number of dowels perpendicular to the frame plane	Deflection in the middle of the beam [mm]
1	1	3.766
2	1	2.972
1	2	3.247
2	2	2.656

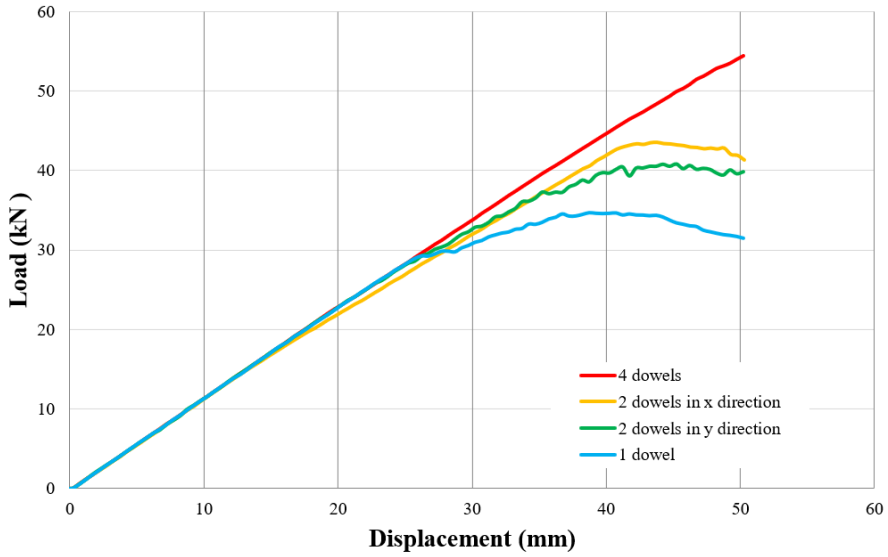

Figure 22. Load-displacement diagrams – in case of different number and position off the dowels

The number of pieces and the geometric arrangement of the dowels have an effect on the deflection of the beam (see Fig. 22), while changing the diameter of the rebar dowel has no effect on the deformation of the beam. By using one dowel, the deflection measured (in the middle cross-section of the beam) in the beam axis (global Z-direction displacement) is 29.5% greater than by using four dowels (see Table 11). The rotating ability of the connection is less affected by dowels placed perpendicularly to the frame plane. However, the dowels spaced in the frame plane significantly affect the rotation of the connection: with dowels spaced one behind the other, the essentially articulated connection can become a moment resistant connection.

In the following, the results for the infill grout/concrete around the rebar dowels are described in detail. There was no crack in the filling concrete until the vertical load was applied. The stress pattern of the same size and distribution was obtained for the models with different material characteristics, while a large amount of cracks were formed in this element. The stresses and cracks were concentrated at the contact surface of the beam and the infill, on the side facing the load at the bottom of the beam. In case of the different material models the same behavior was numerically detected. One notable exception was the model made with the material characteristics of Sikagrout. This model developed a lower stress level than the models made with concrete; see Fig. 23.

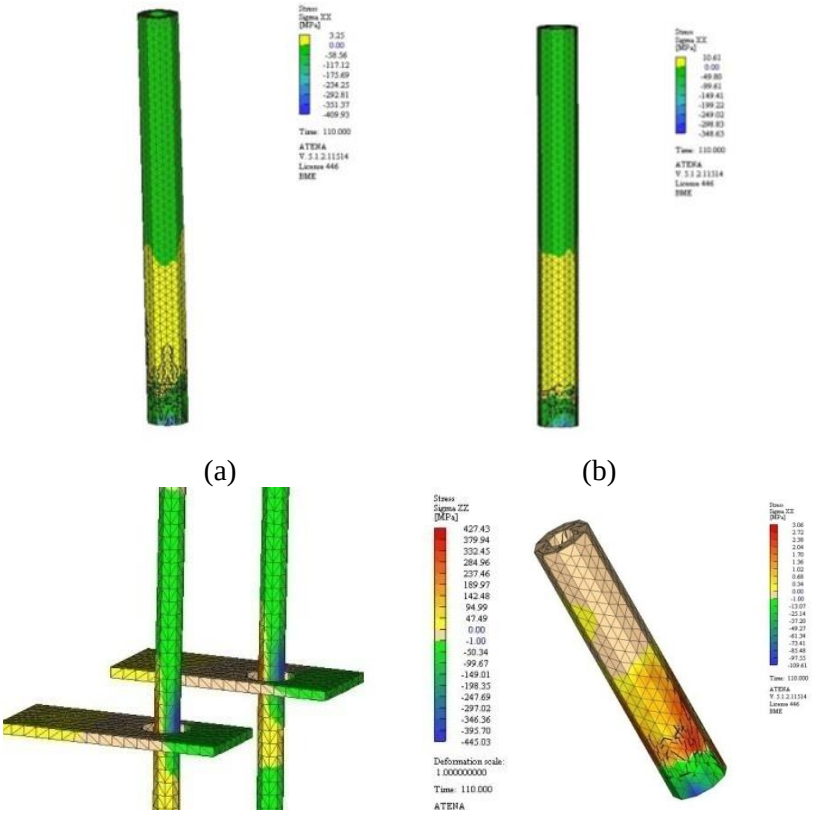

Figure 23. Stresses and crack in the filling concrete a C40/50; b Sikagrout; c double dowels; d singles dowel

The stresses in the infill grout did not change significantly as a result of the change in the number of rebar due to the displacement-controlled test. The eccentrically placed rebar dowels had the greatest effect on the stresses in the filling concrete (see Fig. 21), but had no influence on the behavior of the global structure.

In the following we present the results for the load distribution neoprene sheet. As a result of continuous load increase, different stress distributions were observed in the neoprene sheet. The normal stresses were symmetrical in both main directions (maximum compressive stress 2.45 MPa) approximately in the first third of the load history (load steps 1-10.). Perpendicularly to the frame, the stress distribution was symmetrical only at the first 10 load steps. In the middle of the load history (70th load step) the deflection at the middle cross-section of the beam also increased (4.63 mm at the 70th load step); however, the tractrix of the external load equaled to the longitudinal axis of the beam. At the same time, the compressive normal stresses of the neoprene sheet, longitudinal to the beam, were asymmetrically changed – increased – because of the rotation of the beam end. Finally, at the end of the defined load steps (110th load step), the end of the beam was already angularly turned for the support, so the neoprene sheet was not compressed on its full surface (tension was not allowed between the different elements); see Fig. 24. The numerical model perfectly describes the structural behavior.

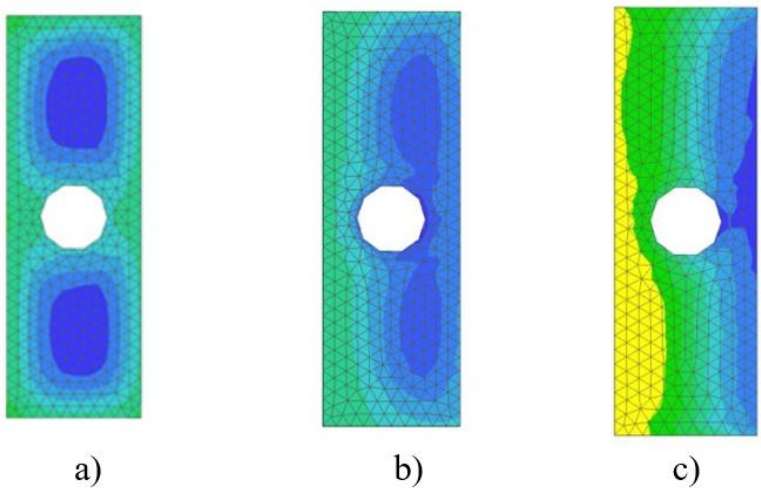

Figure 24. Stress figures on the neoprene sheet a in the 10. load step; b in the 70. load step, c in the 110. load step

The width of the modeled neoprene sheet also has an effect on the midspan deflection of the beam, the principal stresses generated in the sheet, and the compression of the sheet; see Table 12. Deformations were also generated in the plate perpendicular to the direction of the horizontal load (perpendicular to the frame plane) due to the transverse contraction shown in the deformation diagram. See Fig. 25.

Table 12: Comparison of the results in case of different sizes of neoprene sheet in the 10. load step

Width of the neoprene sheet [cm]	Midspan deflection of the beam [mm]	Maximal compression stress in the neoprene sheet [MPa]	Deformation of the neoprene sheet [mm]
10	1.883	2.45	0.3752
20	1.725	1.39	0.1423
Difference (%)	**8.40**	**43.27**	**62.07**

a) b) c)

Figure 25. Deformations of the neoprene sheet a in the 10. load step; b in the 70. load step, c in the 110. load step

In the case of the column, we only deal with the results concerning the end cross-section due to the geometric design of the models. Under the effect of a vertical load, the shape of the neoprene plate is drawn in the end cross-section of the column, which clearly shows the load transfer between the elements and the proper operation of the connection; see Fig. 26. By increasing the width of the plate, it is more difficult to find out about the position of the plate so clearly on the stress diagrams, so the geometry of the connected (modeled) neoprene plate is also important for the column.

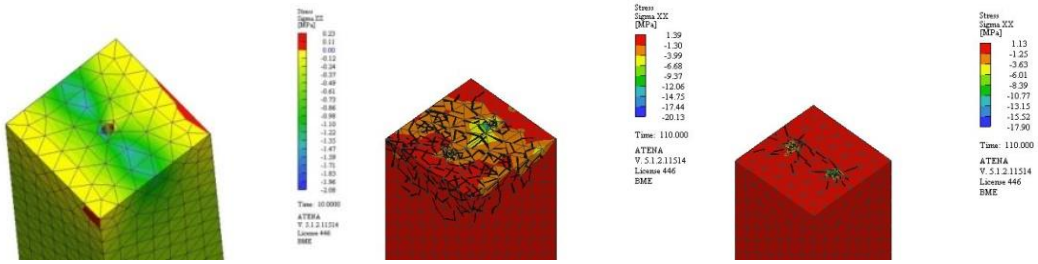

(a) (b) (c)

Figure 26. Stresses at the column end a in the 10. load step; b dowels in ‘y’ direction; c dowels in ‘x’ direction

The horizontal (in plane of frame) stresses and crack images in the end cross section are greatly influenced by the number of placed dowels and their geometric design. The stress concentration developed at the junction of the column and the dowel as expected, but this compressive stress did not reach the characteristic value of the compressive strength of the concrete in any of the models (maximum compressive stress 20.16 MPa), see on Fig. 26.

When modeling the total frame skeleton, we found that the force-top displacement diagram of the structure differs from the other models. The complete ATENA 3D frame model was constructed based on the experience regarding the foundation connection. The model was made with a 30 * 50 cm beam cross section, 2 dowels (perpendicular to the frame plane), C40 / 50 filling concrete and a 10 cm wide neoprene plate. The foundation part was designed according to the "O30-KM75-KA25" model (30*30 cm column size, 75 cm height of filling concrete and C25/30 filing concrete material). After a horizontal displacement of nearly 7.00 mm, the slope of the diagram greatly decreased until the peak force of 24.54 kN (displacement: 50.66 mm); see Fig. 27. Compared to the whole ATENA 3D model, it can be stated that at the same load level (peak force: 24.54 kN) the Axis VM model yields significantly smaller displacements (comparing displacements is almost meaningless). In this model, we obtained a similar stress distribution in the element of the connection as before; however, due to the softer behavior, a lower stress (109 MPa compressive stress in the infill concrete) developed at the end of the loading process in each element than in the "joint" models. The position of the cracks is also the same as shown by the previous results: their density decreased (see Fig. 28). Overall, the global ATENA 3D frame model describes the behavior of the structure as expected, but for a more accurate analysis, it is essential to compare the numerical results obtained by laboratory results.

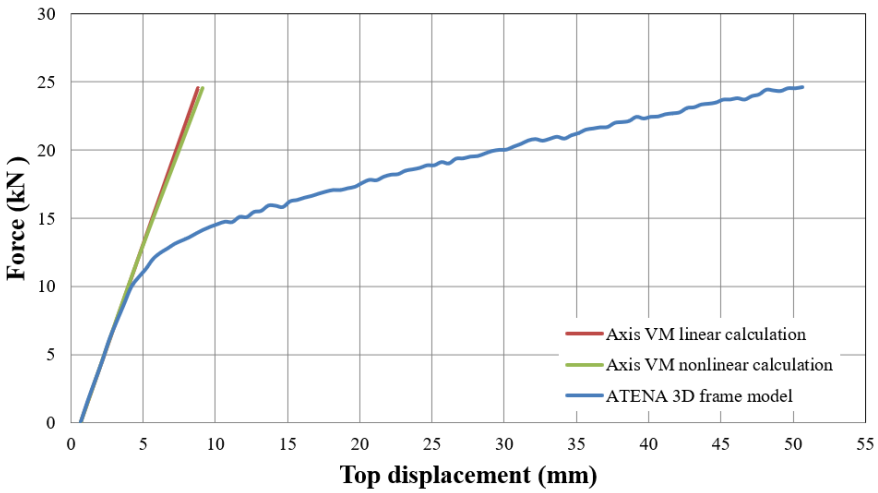

Figure 27. Load-displacement diagram – in case of modeling the whole frame skeleton

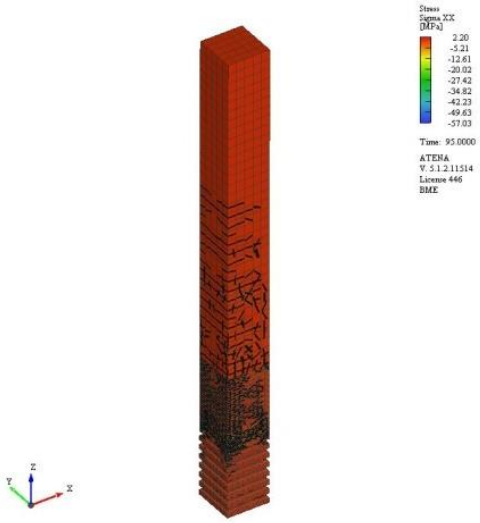

Figure 28. Stress figure in the 110. load step

4. CONCLUSIONS

In this article, we examined the behavior of a cup foundation-column and beam-column joints of a simple frame skeleton. We changed the parameters of the spatial model of the presented column-cup foundation and beam-column connections, and then we compared the force-displacement and stress results obtained during the linear and nonlinear-based studies, highlighting the differences between the two methodologies. Our non-linear studies were performed with a non-linear finite element software (ATENA 3D) developed specifically for the numerical studies of concrete and reinforced concrete structures, in which we used the modeling procedure / technique we developed earlier (Haris, Roszevák 2017; Roszevák, Haris 2019). Furthermore, we compared the differences in the results of the models of different designs, taking into account the force-displacement diagrams, deformations, the resulting stress distributions, and their values.

Based on the numerical tests we performed, we make the following findings:

Column-cup foundation connection:

- Numerically, a reduction of ~ 28.27 % is caused by the decrease in the height of the filling concrete in the cup foundation. At the same load level (1.91 kN), there is a difference of almost 1.70-2.46 % between the Axis VM and the Atena 3D models.
- In contrast, for all three column sizes, it can be observed that as the height of the filling concrete decreases, the horizontal reaction force also decreases by nearly 15-19% (between the KM75 and KM25 models).
- With regard to the displacements associated with peak force, the results are already significantly different, ranging from 16% to 32%, depending on the filling concretes of different heights and the cross-sections of the column.
- Based on the results obtained with the created models, it will be possible to analyze the energy dissipated by the structure in a later research program. Furthermore, based on the

results obtained, it can be stated that the height of the filling concrete formed during construction can have a significant effect on the behavior of the structure, so it must / can be duly taken into account during the design of the structure.

- The results show that the change in the material quality of the filling concrete in the column-cup foundation connections does not have a significant effect on the horizontal force at the monitoring point of the models: the largest difference is ~ 1% for the O40-KM25 models.
- The results show that shrinkage modeling with shrinkage deformation affects the global behavior of the structure. Failure occurs at nearly equal horizontal force levels (with shrinkage: 12.02 kN; without shrinkage: 12.23 kN), but the displacement associated with these values increases by nearly 6.09% (with shrinkage: 98.40 mm; without shrinkage: 92.40 mm).
- In examining the peak force, the ribbed model is able to absorb nearly 10% more force, with deformations increasing by only 1.8 % compared to the results obtained using models of cup foundation modeled with a flat inner surface.
- Based on our investigations, the supporting effect of the soil can be modeled; however, the models that take into account the actual soil stratification can be examined in further research programs.

Column-beam connection:

- The results shown that the deflections obtained in the Axis VM exceed nearly 32 % in the case of the 30*50 beam cross section.
- The deflections belonging to Axis VM are 32.28 % (ATENA 3D straight beam) and 47.93 % (ATENA 3D notched ended beam) smaller. Overall, we can say that the depth of the computational technique and the form of the beam end greatly influence the deformations of the beam.
- The number of pieces and the geometric arrangement of the dowels have an effect on the deflection of the beam, while changing the diameter of the rebar dowel has no effect on the deformation of the beam.
- By using one dowel, the deflection measured (in the middle cross-section of the beam) in the beam axis (vertical displacement) is 29.5% greater than by using four dowels. The rotating ability of the connection is less affected by dowels placed perpendicularly to the frame plane.
- The stresses in the infill grout did not change significantly as a result of the change in the number of rebar due to the displacement-controlled test.
- The eccentrically placed rebar dowels had the greatest effect on the stresses in the filling concrete, but had no influence on the behavior of the global structure.
- The width of the modeled neoprene sheet also has an effect on the midspan deflection of the beam (8.40 % bigger deflection in case of 10 cm width). Regarding the deformations of the neoprene sheet the numerical model perfectly describes the structural behavior.
- In the case of the column, we only deal with the results concerning the end cross-section due to the geometric design of the models. The geometry of the connected (modeled) neoprene plate is also important for the column.

- Compared to the whole ATENA 3D model, it can be stated that at the same load level (peak force: 24.54 kN) the Axis VM model yields significantly smaller displacements (comparing displacements is almost meaningless). Overall, the global ATENA 3D frame model describes the behavior of the structure as expected, but for a more accurate analysis, it is essential to compare the numerical results obtained by laboratory results.

In summary, with the modeling technique we developed, the prefabricated reinforced concrete column-cup and column-beam connection can be examined in detail by using ATNEA 3D nonlinear finite element software. The results obtained shed light on the fact that there may be significant differences between simpler finite element calculations and higher-level finite element calculations. Furthermore, it is clear that simplifications made in everyday design practice can have a very large impact on the whole structure or individual structural elements and the quality of construction and its implementation is not a negligible aspect from the point of view of the design of the structure.

Compliance with ethical standards

Conflict of interest On behalf of the authors, the corresponding author states that there is no conflict of interest.

REFERENCES

1. Arthi S, Jaya KP. Experimental study on shear behaviour of precast shear wall-slab dowel connection, *Asian J Civil Eng* 2020; **21**: 663-76. https://doi.org/10.1007/s42107-020-00229-z.
2. Ashida KM, Yedhu K. Analytical study on seismic stability of different foundation connection, *Int Res J Adv Eng Sci* 2017; **2**(2): 203-9.
3. Ashtiani MS, Dhakal RP, Scott AN. Cyclic response analysis of high-strength self-compacting concrete beam-column joints: Numerical modelling and experimental validation, *Bullet New Zealand Societ Earthq Eng* 2018; **51**(1): 23-33.
4. Brunesi E, Nascimbene R, Bolognini D, Bellotti D. Experimental investigation of the cyclic response of reinforced precast concrete framed structures, *PCI J* 2015; **60**(2): 57-79. https://doi.org/10.15554/pcij.03012015.57.79
5. Cervenka V. Constitutive model for cracked reinforced concrete, *ACI J* 1985; **82**(6): 877-82.
6. Cervenka, V, Jendele L, Cervenka J. *Atena Program Documentation Part 1, Theory*, Cervenka Consulting s.r.o, 19, 2014.
7. Collins MP, Mitchell D. Shear and torsion design of prestressed and non-prestressed concrete beams, *PCI J* 1980; **25**(5): 32-100. https://doi.org/10.15554/pcij.09011980.32.100
8. Cheok GS, Lew HS (). Performance of precast concrete beam-to-column connections subject to cyclic loading, *PCI J* 1991; **36**(3): 56-67. https://doi.org/10.15554/pcij.05011991.56.67
9. Crisfield MA, Wills J. The analysis of reinforced concrete panels using different concrete models, *J Eng Mech, ASCE* 1989; **115**(3): 578-97.

10. Darwin D, Pecknold DAW. *Inelastic Model for Cyclic Biaxial Loading of Reinforced Concrete*, Civil Engineering Studies, University of Illinois, July, 1974.
11. Pryl D, Červenka J. *ATENA Program Documentation, Part 11: Troubleshooting Manual*, Cervenka Consulting s.r.o, 19, 2014.
12. Fediuc DO, Budescu M, Fediuc V, Venghiac VM. Compression modulus of elastomers, Buletinul Insitutului Politehnic Din Iasi, Universitaea Tehnica "Gheirge Asachi" din Iasi, Tomul LIX (LXIII), 2013.
13. Fediuc DO, Budescu M, Venghiac VM. The behavior under compression of elastomers used in base isolation bearings, Buletinul Insitutului Politehnic Din Iasi, Universitaea Tehnica "Gheirge Asachi" din Iasi, Tomul LIX (LXIII), 2013.
14. Féd. Int. du Béton: *Planning and Design Handbook on Precast Building Structures*, Bulletin 74.
15. *Fib Model Code for Concrete Structures*, 2010, Wilhelm Ernst & Sohn, Berlin, 2013.
16. Gaston JR., Kriz LB. Connections In Precast Concrete Structures – Scarf Joints, *PCI J* 1964; **9**(3): 37-59. https://doi.org/10.15554/pcij.11011980.38.61
17. Guerrero H, Rodriguez V, Escobar JA, Alcocer SM, Bennetts F, Suarez M. Experimental ttest of precast reinforced concrete beam-column connections, *Soil Dyn Earthq Eng* 2019; **125**: 105743. https://doi.org/10.1016/j.soildyn.2019.105743.
18. Haris I, Roszevák Zs. Numerical and experimental analysis of prefabricated reinforced concrete beams, *Vasbetonépítés: A FIB Magyar Tagozat Lapja: Műszaki Folyóirat* 2017; **19**(1): 2-11.
19. Hawileh RA, Rahman A, Tabatabai H. Nonlinear finite element analysis and modeling of a precast hybrid beam-column connection subjected to cyclic loads, *Appl Mathemat Modell* 2010; **34**(9): 2562-83.
20. Hooper CD. Low-temperature elastic behavior of fourteen compounded elastomers, *NASA Tech Memorand* 1964, NASA TM X-53137.
21. Hordijk DA. Local Approach to Fatigue of Concrete, Doctor dissertation, Delft University of Technology, The Netherlands, ISBN 90/9004519-8, 1991.
22. Kaveh A, Hosseini SM, Akbari H. Efficiency of plasma generation optimization for structural damage identification of skeletal structures based on a hybrid cost function, *Iran J Sci Technol Trans Civil Eng* 2020, https://doi.org/10.1007/s40996-020-00504-8.
23. Kaveh A, Hosseini SM, Zaerreza A. Size, layout, and topology optimization of skeletal structures using plasma generation optimization, *Iran J Sci Technol Trans Civil Eng* 2020, https://doi.org/10.1007/s40996-020-00527-1.
24. Kiss Z. Precast concrete frame buildings with rigid connections in areas with high seismic activity, *Vasbetonépítés: A FIB Magyar Tagozat Lapja: Műszaki Folyóirat* 2018; **20**(2): 26-35. DOI: 10.32969/VB.2018.2.1.
25. Kolmar W. Beschreibung der Kraftuebertragung über Risse in nichtlinearen Finite-Element-Berechnungen von Stahlbetontragwerken, Dissertation, T.H. Darmstadt, 1986, pp. 94.
26. Krishnan T, Purushothaman R. Development and testing of damage controllable precast beam-column connection under reverse cyclic loading, *Asian J Civil Eng* 2020; **21**: 1343-54. https://doi.org/10.1007/s42107-020-00281-9.
27. Kupfer H, Hilsdorf HK, Rüsch H. Behavior of concrete under biaxial stress, *ACI Jo* 1969; **66**(8): 656-66.

28. Pall AS, Marsh C, Fazio P. Friction joints for seismic control of large panel structures, *PCI J* 1980; **25**(6): 38-61. https://doi.org/10.15554/pcij.11011980.38.61.
29. Priya et al. Analytical investigation on the seismic behaviour of precast pocket foundation connection, *Int Res J Advanc Eng Sci* 2016; **7**(1): 214-8.
30. Roszevák Zs, Haris I. Finite element analysis of cast-in-situ RC frame corner joints under quasi static and cyclic loading, *Revista de la Construct* 2019; **18**(3): 579-94.
31. Tullini N, Minghini F. Cyclic test on a precast reinforced concrete column-to-foundation grouted duct connection, *Bull Earthq Eng* 2020; **18**: 1657-91. https://doi.org/10.1007/s10518-019-00766-2
32. Van Mier JGM. Multi-axial Strain-softening of Concrete, Part I: fracture, *Mater Struct* 1986; *RILEM*, **19**(111).
33. Vecchio FJ, Collins MP. Modified compression-field theory for reinforced concrete beams subjected to shear, *ACI J* 1986; **83**(2): 219-31.
34. Vidjeapriya R, Jaya KP. Experimental study on two simple mechanical precast beam-column connections under revers cyclic loading, *J Perform Construct Facilit* 2013; **27**(4): 402-14. https://doi.org/10.1061/(ASCE)CF.1943-5509.0000324.
35. Zhang J, Ding Ch, Rong X, Yang H, Wang K, Zhang B. Experimental seismic study of precast hybrid SFRC/RC beam-column connections with different connection details, *Eng Struct* 2020; **208**: 110-295. https://doi.org/10.1016/j.engstruct.2020.110295.